

KCTD1 mutants in scalp-ear-nipple syndrome and AP-2 α P59A in Char syndrome reciprocally abrogate their interactions, but can regulate Wnt/ β -catenin signaling

LINGYU HU¹, LI CHEN², LIU YANG², ZI YE³, WENHUAN HUANG²,
XINXIN LI², QING LIU², JUNLU QIU² and XIAOFENG DING²

¹Department of Obstetrics and Gynecology, Third Xiangya Hospital of The Central South University, Changsha, Hunan 410013; ²Key Laboratory of Protein Chemistry and Development Biology of State Education Ministry of China, College of Life Science, Hunan Normal University, Changsha, Hunan 410081; ³Yali High School of Changsha, Changsha, Hunan 410007, P.R. China

Received June 19, 2019; Accepted July 14, 2020

DOI: 10.3892/mmr.2020.11457

Abstract. Potassium-channel tetramerization-domain-containing 1 (KCTD1) mutations are reported to result in scalp-ear-nipple syndrome. These mutations occur in the conserved broad-complex, tramtrack and bric a brac domain, which is associated with inhibited transcriptional activity. However, the mechanisms of KCTD1 mutants have not previously been elucidated; thus, the present study aimed to investigate whether KCTD1 mutants affect their interaction with transcription factor AP-2 α and their regulation of the Wnt pathway. Results from the present study demonstrated that none of the ten KCTD1 mutants had an inhibitory effect on the transcriptional activity of AP-2 α . Co-immunoprecipitation assays demonstrated that certain mutants exhibited changeable localization compared with the nuclear localization of wild-type KCTD1, but no KCTD1 mutant interacted with AP-2 α . Almost all KCTD1 mutants, except KCTD1 A30E and H33Q, exhibited differential inhibitory effects on regulating TOPFLASH luciferase reporter activity. In addition, the interaction region of KCTD1 to the PY motif (amino acids 59-62) in AP-2 α was identified. KCTD1 exhibited no suppressive effects on the transcriptional activity of the AP-2 α P59A mutant, resulting in Char syndrome, a genetic disorder characterized by a distinctive facial appearance, heart defect and hand abnormalities, by altered protein cellular localization that abolished protein interactions. However, the P59A, P60A, P61R and 4A AP-2 α

mutants inhibited TOPFLASH reporter activity. Moreover, AP-2 α and KCTD1 inhibited β -catenin expression levels and SW480 cell viability. The present study thus identified a putative mechanism of disease-related KCTD1 mutants and AP-2 α mutants by disrupting their interaction with the wildtype proteins AP-2 α and KCTD1 and influencing the regulation of the Wnt/ β -catenin pathway.

Introduction

Scalp-ear-nipple (SEN) syndrome is a rare, autosomal-dominant disorder that commonly presents as cutis aplasia of the scalp, minor anomalies of the external ears, digits and nails, and malformation of the breast (1). In mice, homozygous deficiency of the lymphoid enhancer-binding factor 1 (Lef-1) gene results in the lack of whiskers and the arrest of hair-follicle development, lack of mammary glands and edentulism, indicating that Lef-1 may serve as a potential candidate gene for treating SEN syndrome (2). Ten mutations in the broad-complex, tramtrack and bric a brac (BTB) domain of potassium-channel tetramerization-domain-containing 1 (KCTD1) have been identified in ten families with SEN syndrome of European, Brazilian and North African background (3). This conserved domain regulates transcriptional activity, suggesting it may serve a key role in KCTD1 protein function during ectodermal development (3).

Transcription factor AP-2 α -knockout mice exhibit a number of severe developmental phenotypes, including neural tube, body wall and craniofacial abnormality (4). Dominant AP-2 α mutant Doarad results in a missense mutation that affects the Y⁵⁸F⁵⁹P⁶⁰P⁶¹P⁶²Y⁶³ (PY) motif in the transactivation domain of AP-2 α , causing a misshapen malleus, incus and stapes (5). This P59L mutation in AP-2 α leads to increased transcriptional activation of AP-2 α (5). Patients with Char syndrome have three mutations in the basic DNA-binding domain and a PY motif in the activation domain of the AP-2 β gene, causing dominant-negative effects. In the USA, individuals with Char syndrome who have a PY motif P62R mutation in AP-2 β have a higher incidence rate (10 of 14) of

Correspondence to: Professor Xiaofeng Ding, Key Laboratory of Protein Chemistry and Development Biology of State Education Ministry of China, College of Life Science, Hunan Normal University, Building 2, 36 Lushan Road, Changsha, Hunan 410081, P.R. China
E-mail: fengxiaoding@hotmail.com

Key words: potassium-channel tetramerization-domain-containing 1, AP-2 α , β -catenin, mutation

patent ductus arteriosus, but milder hand and facial abnormal phenotypes compared with individuals with DNA-binding domain mutations in AP-2 α (6,7). Point mutations or insertions/deletions in the conserved DNA-binding domain in AP-2 α , encoded by exons 4 and 5, cause the majority of branchio-oculo-facial syndrome (BOFS) cases (8). BOFS is associated with >25 different mutations in AP-2 α (9-12). Therefore, AP-2 α mutants have been associated with certain developmental abnormalities.

Our previous study (13) demonstrated that KCTD1 binds with AP-2 α and decreases its transcriptional activity. KCTD15 is associated with the KCTD1 protein in the KCTD family. It is likely that KCTD15 functions during embryogenesis by interacting with the activation domain of AP-2 α to inhibit neural crest induction (14). Individuals with KCTD15 mutations exhibit developmental defects in neural crest derivatives and the torus lateralis (TLa) in the central nervous system, resulting in a significant decrease in normal growth rates (15,16). Moreover, both AP-2 α and KCTD1 regulate the Wnt/ β -catenin pathway. AP-2 α directly interacts with adenomatous polyposis coli (APC), stabilizing interactions between APC and β -catenin, attenuating interactions between β -catenin and transcription factor-4 in the nucleus and suppressing TOPFLASH luciferase reporter activity in human colorectal cancer cells (17). AP-2 α -interacting protein KCTD1 directly binds to β -catenin, enhances β -catenin ubiquitination and degradation, which is dependent on casein kinase 1/glycogen synthase kinase-3 β -mediated phosphorylation of β -catenin, and inhibits the canonical Wnt/ β -catenin signaling pathway (18).

The present study aimed to investigate whether KCTD1 and AP-2 α protein mutants reciprocally regulate their interactions and inhibit the Wnt/ β -catenin signaling pathway. The results demonstrated that BTB domain mutations in KCTD1 were not associated with AP-2 α . The P59A mutation in the PY motif of AP-2 α prevented binding with KCTD1, but the majority of BTB domain mutations in KCTD1 and PY motif mutations in AP-2 α resulted in inhibited Wnt pathway-responsive TOPFLASH reporter gene expression levels. Wild-type KCTD1 suppressed the transcriptional activity of AP-2 α P60A and P61R to repress TOPFLASH reporter gene expression levels. Moreover, wild-type KCTD1 and AP-2 α downregulated β -catenin expression levels and decreased the viability of SW480 cells. These findings highlighted the importance of AP-2 α and KCTD1 regulation in maintaining a normal tissue phenotype.

Materials and methods

Plasmid generation. Recombinant overexpressing plasmids pCMV-Myc-AP-2 α , pCMV-HA-KCTD1, pCMV-Myc-KCTD1 and pEGFP-C1-AP-2 α were generated as previously described (13,18). The mutants AP-2 α P61R and KCTD1 P20S, A30E, P31R, H33P and H33Q were also generated as previously described (13,18). The KCTD1 mutants P31L, P31H, G62D, D69E and H74P and AP-2 α mutants P59A, P60A and 4A (P59AP60AP61AY62A) were modified by PCR-based site-directed mutagenesis and cloned into pCMV-Myc plasmids. Mutated primers are presented in Table I. Reporter vectors A2 and TOPFLASH were generated

as previously described (18,19). Eight recombinant plasmids were sequenced using the Sanger method, in order to verify mutant site points (Sangon Biotech, Co., Ltd.) (Fig. S1).

Cell culture and transfection. SW480, 293 and HeLa cells (American Type Culture Collection) were cultured in complete DMEM (Sigma-Aldrich; Merck KGaA). All cells were maintained with 10% fetal calf serum (HyClone; GE Healthcare Life Sciences), 2 mM glutamine, 10 U/ml penicillin and 100 μ g/ml streptomycin at 37°C with 5% CO₂. The cells were transiently transfected with different amounts of plasmid DNA (1 μ g for luciferase reporter assays; 6 μ g for immunofluorescence analysis; 20 μ g for co-immunoprecipitation; Clontech Laboratories, Inc.) using Lipofectamine[®] 2000 reagent (Invitrogen; Thermo Fisher Scientific, Inc.) for 6 h. The cells were collected 24-30 h following transfection for subsequent experimentation.

Luciferase reporter assays. The 293 cells were cultured and transiently transfected with 0.3 μ g reporter plasmids A2 (generous gift of Professor Trevor Williams) or pTOPFLASH (Clontech Laboratories, Inc.) (18) and the indicated plasmids (0.3 μ g pCMV-Myc-KCTD1 and/or 0.3 μ g of pCMV-Myc-AP-2 α) in 12-well plates using Lipofectamine 2000 reagent as previously described (20). Briefly, 0.1 μ g pCMV-LacZ plasmid (19) was co-transfected in each well to measure transfection efficiency as an internal β -galactosidase control. The total amount of 1 μ g plasmid DNA in each well was maintained by adding empty vector pCMV-Myc (Clontech Laboratories, Inc.) to each transfection. β -galactosidase and luciferase activities were assessed 24 h after transfection using a Promega Luciferase Assay system (Promega Corporation) and a Turner TD20/20 luminometer (Turner Designs). The luciferase activity is normalized relative to the β -galactosidase control. A total of three experimental repeats were performed.

Immunofluorescence localization analysis. HeLa cells were grown to ~70% confluence on glass coverslips and transiently transfected with 3 μ g GFP-AP-2 α and 3 μ g Myc-KCTD1 mutants or 3 μ g Myc-AP-2 α mutants and 3 μ g HA-KCTD1. At 30 h post-transfection, cells were collected for immunofluorescence staining, as previously described (19). Primary antibodies included Anti-Myc mouse monoclonal antibody (clone. no. 9E10; Santa Cruz Biotechnology, Inc.) and anti-HA rabbit polyclonal antibody (clone no. Y-11) (Santa Cruz Biotechnology, Inc.) at 1:200 dilution for 1 h at 4°C. Alexa Fluor 488 goat anti-rabbit IgG (cat. no. A27034) and Alexa Fluor 594 goat anti-mouse IgG (cat. no. A-11005) secondary antibodies were purchased from Molecular Probes; Thermo Fisher Scientific, Inc. and used at 1:500 dilution for 45 min at 4°C. Hoechst 33258 (1 μ g/ml) was used to stain the nuclei (Sigma-Aldrich; Merck KGaA) for 5 min at 4°C. The fluorescence signals were observed with a fluorescence microscope (Carl Zeiss AG).

Co-immunoprecipitation. The 293 cells were grown to ~80% confluence and transiently transfected with 10 μ g Myc-AP-2 α and 10 μ g Myc-KCTD1 in 10-cm dishes. At 30 h after transfection, cells were collected and lysed as previously described (13). The cells were lysed in RIPA buffer [50 mM

Table I. Mutants of KCTD1 and AP-2 α and their PCR primers.

Gene	Mutant	Primer sequence (5'→3')
KCTD1	P20S	F: <u>T</u> CTACTCCAGCACA <u>A</u> CTCACA R: TGTGAGTTGTGCTGGAGTAG <u>A</u>
	A30E	F: ATCCAATG <u>A</u> GCCTGTCCACAT R: ATGTGGACAGGCTCATTGGAT
	P31R	F: CAATGCGC <u>G</u> TGTCCACATTGA R: TCAATGTGGACAC <u>G</u> CGCATTG
	P31L	F: CAATGCGC <u>T</u> TGTCCACATTGA R: TCAATGTGGACA <u>A</u> GCGCATTG
	P31H	F: CAATGCGC <u>A</u> TGTCCACATTGA R: TCAATGTGGACA <u>T</u> GCGCATTG
	H33P	F: <u>C</u> CATTGATGTGGGCGGCCAC R: GTGGCCGCCACATCAAT <u>G</u> G
	H33Q	F: CGCCTGTCCA <u>A</u> ATTGATGTGG R: CCACATCAAT <u>T</u> TGGACAGGCG
	G62D	F: TTTGATG <u>A</u> TACAGAGCCCATTG R: CAATGGGCTCTGT <u>A</u> TCAATCAA
	D69E	F: <u>A</u> AGTCTCAAACAGCACTATTTTC R: GAAATAGTGCTGTTT <u>G</u> AGACTT
	H74P	F: <u>C</u> CTATTTCATTGACAGAGATGG R: CCATCTCTGTCAATGAAATAG <u>G</u>
AP-2 α	P61R	F: TTCCCCCA <u>A</u> GATACCAGCCT R: AGGCTGGTAT <u>C</u> TGGGGGGAA
	P59A	F: ATACTTC <u>G</u> CCCCACCCTACC R: GGTAGGGTGGGG <u>C</u> GAAGTAT
	P60A	F: ACTTCCCC <u>G</u> CACCCTACCAG R: CTGGTAGGGTGC <u>G</u> GGGAAGT
	4A	F: ATACTTC <u>G</u> CCCGAGCCGCCAGCCT R: AGGCTGGG <u>C</u> GGCTGC <u>G</u> GGCGAAGTAT

F, forward; KCTD1, potassium-channel tetramerization-domain-containing 1; R, reverse. The mutated base is underlined.

Tris-HCl pH 7.2; 150 mM NaCl, 1% (v/v) Triton X-100; 1% (w/v) sodium deoxycholate; 0.1% (w/v) SDS] supplemented with protease inhibitors. The cellular lysates were precleared with protein A/G plus agarose (Santa Cruz Biotechnology, Inc.) at 4°C for 1 h, and then immunoprecipitated using rabbit anti-KCTD1 polyclonal antibodies (21) and protein A/G plus agarose. The immunoprecipitates were washed four times for 15 min each in 1 ml 1% Triton buffer by keeping gentle agitation and then centrifuged at 500 x g for 3 min at 4°C. The immunocomplexes were separated by SDS-PAGE on 13% gels and detected with mouse anti-Myc tag monoclonal antibody at 1:2,000 dilution overnight at 4°C as described in the following Western blot section. Pre-immune rabbit IgG (cat. no. sc-2027; Santa Cruz Biotechnology, Inc.) was used as a negative control. The quantification of immunoprecipitated bands was analyzed using ImageJ software (ImageJ 1.48v, <https://imagej.nih.gov/ij/>).

Western blotting. SW480 cells were transiently transfected with pCMV-Myc-AP-2 α and/or pCMV-Myc-KCTD1

expression plasmids. At 24 h after post-transfection, cells were collected and lysed in RIPA buffer. The protein concentration of whole-cell extracts was measured using a BCA assay kit (Pierce; Thermo Fisher Scientific, Inc.). Total protein (10 μ g/lane) was resolved by SDS-PAGE on 12% gels, then transferred to PVDF membranes (Bio-Rad Laboratories, Inc.) at 4°C for 2 h at 100 V. The membrane was blocked with TBS buffer [100 mM Tris-HCl pH7.5; 0.9% (w/v) NaCl] with 1% BSA (Sigma-Aldrich; Merck KGaA) for 1 h at 4°C. After blocking, the membrane was incubated with primary antibodies against Myc-tag (clone. no. 9E10; 1:2,000), β -catenin (E-5, 1:1,000), cyclin D1 (CCND1; clone. no. HD11; 1:1,000) and GAPDH (clone. no. 6C5; 1:5,000) (Santa Cruz Biotechnology, Inc.) overnight at 4°C and washed with TBS and 0.1% (v/v) Tween-20 for 1 h. After washing, the membrane was then incubated with goat anti-mouse IgG-horseradish peroxidase-conjugated secondary antibody (cat. no. sc-2005, 1:7,500; Santa Cruz Biotechnology, Inc.) at room temperature for 45 min followed by washing five times for 1 h. The signal was detected with SuperSignal West Pico chemiluminescent Substrate (Pierce; Thermo Fisher Scientific, Inc.) and visualized with tanon-5200 system (Tanon Science and Technology Co., Ltd.).

Cell viability assays. A total of 3x10³ transfected SW480 cells were grown at 37°C in 96-well plates in octuplicate. Cell viability was analyzed 24 h after transfection by adding 1 mg/ml MTT to each well, followed by incubation for 4 h at 37°C. Subsequently, the formazan crystals were dissolved in 100 μ l DMSO. The absorbance was measured at 490 nm using a spectrophotometer. To detect the effects of AP-2 α and KCTD1 proteins on the sensitivity of SW480 cells to sorafenib, SW480 cells were transfected and subsequently treated with 20 μ M cisplatin (DDP) for 24 h; viability was assessed by MTT, aforementioned.

Statistical analysis. All statistical analysis was performed using SPSS statistical software (version 16.0; SPSS, Inc.). Data are presented as the mean \pm SD of three independent experiments. Significant differences were determined using Student's t-test to compare two groups, and two-way ANOVA to compare three or more groups. Multi-group comparisons were analyzed using Tukey's post hoc test. P<0.05 was considered to indicate a statistically significant difference.

Results

Known KCTD1 mutants have no inhibitory effect on the transcriptional activity of AP-2 α , and KCTD1 does not repress the transcriptional activity of the AP-2 α P59A mutation. All the known KCTD mutations in the BTB-domain lead to SEN syndrome, whereas mutations in AP-2 α possibly cause Char syndrome. As the BTB domain of KCTD1 binds to the activation domain of AP-2 α and suppresses its transcriptional activity (13), it was investigated whether these KCTD1 mutations affect AP-2 α transcriptional activity (Fig. 1A). An A2 reporter plasmid with three AP-2 binding sites was transiently transfected in the presence or absence of pCMV-Myc-KCTD1 wild-type or KCTD1 mutants into 293 cells. Consistent with previous results (13) wild-type KCTD1 overexpression significantly decreased A2 luciferase activity,

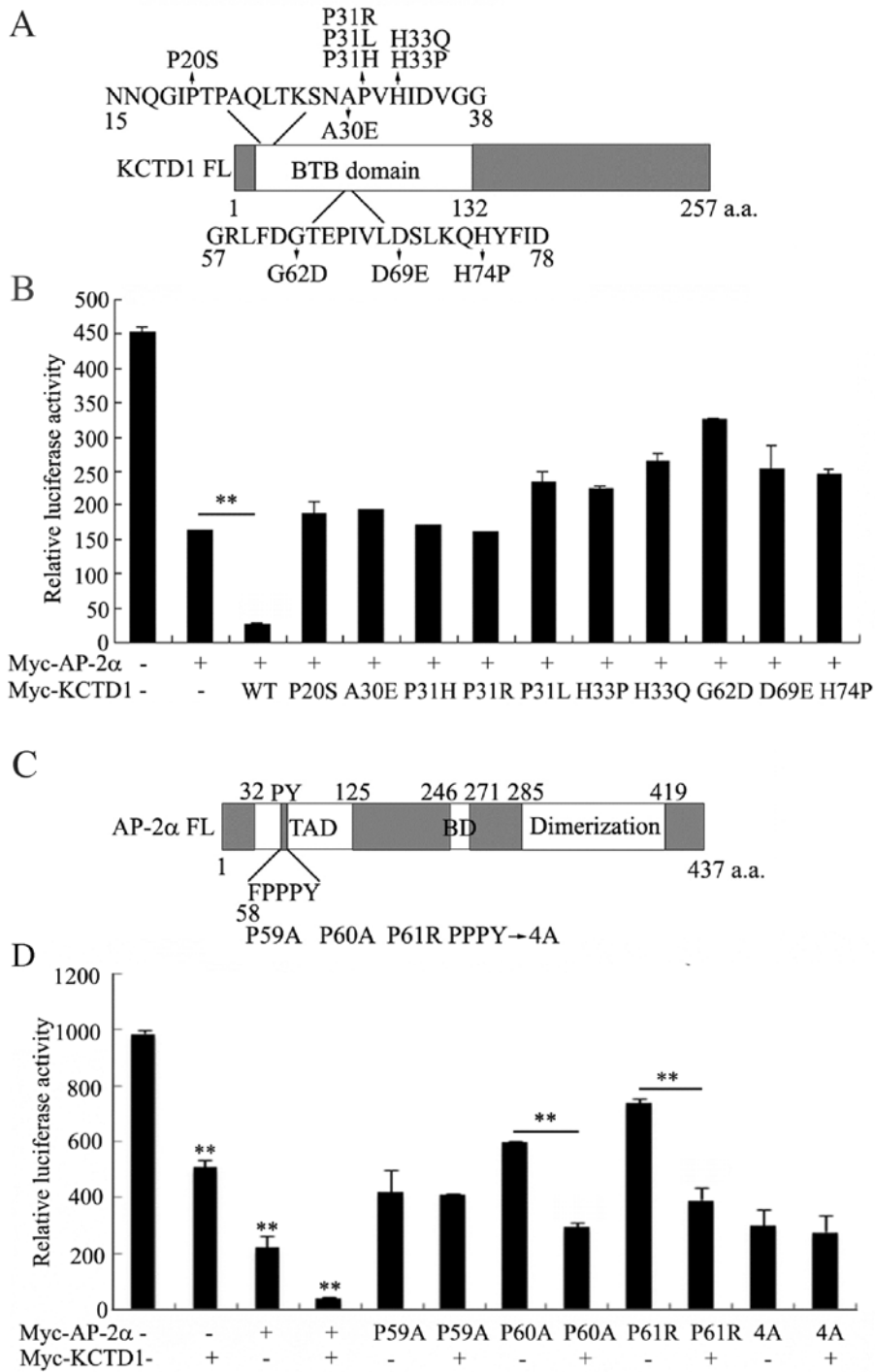


Figure 1. Effects of KCTD1 and AP-2 α mutants on A2 luciferase reporter activity. (A) Schematic diagram showing the domain structure of KCTD1 and mutants associated with scalp-ear-nipple syndrome. (B) 293 cells were transiently transfected with A2 luciferase reporter vector, AP-2 α alone or in combination with either wild-type KCTD1 or KCTD1 mutants. (C) Schematic diagram showing the domain structure of AP-2 α and mutants associated with Char syndrome. (D) Transfection was performed with the A2 reporter vector in the presence or absence of KCTD1 or with KCTD1 co-transfected with either wild-type AP-2 α or AP-2 α mutants in 293 cells. At 24 h after transfection, luciferase and β -galactosidase activities were determined. Relative luciferase activity is expressed as the mean \pm SD of three independent experiments normalized to β -galactosidase activity. **P<0.01. FL, full-length; TAD, transactivation domain; BD, DNA-binding domain; BTB, broad-complex, tramtrack and bric a brac domain; DIM, dimerization domain; KCTD1, potassium-channel tetramerization-domain-containing 1.

whereas 10 KCTD1 mutants had no effect on the transcriptional inhibition of AP-2 α , compared with wild-type KCTD1 (Fig. 1B).

The present study also investigated the effect of KCTD1 on the transcriptional activity of AP-2 α with mutations in the PY motif (Fig. 1C), which is required for a normal developmental

phenotype (5). KCTD1 markedly repressed A2 luciferase activity of AP-2 α P60A and P61R, but not of AP-2 α P59A or 4A, indicating that the AP-2 α mutation of amino acid 59 abrogated KCTD1 regulation (Fig. 1D). Taken together, these data revealed that pathogenic mutations in KCTD1 or AP-2 α affect their regulatory mechanisms.

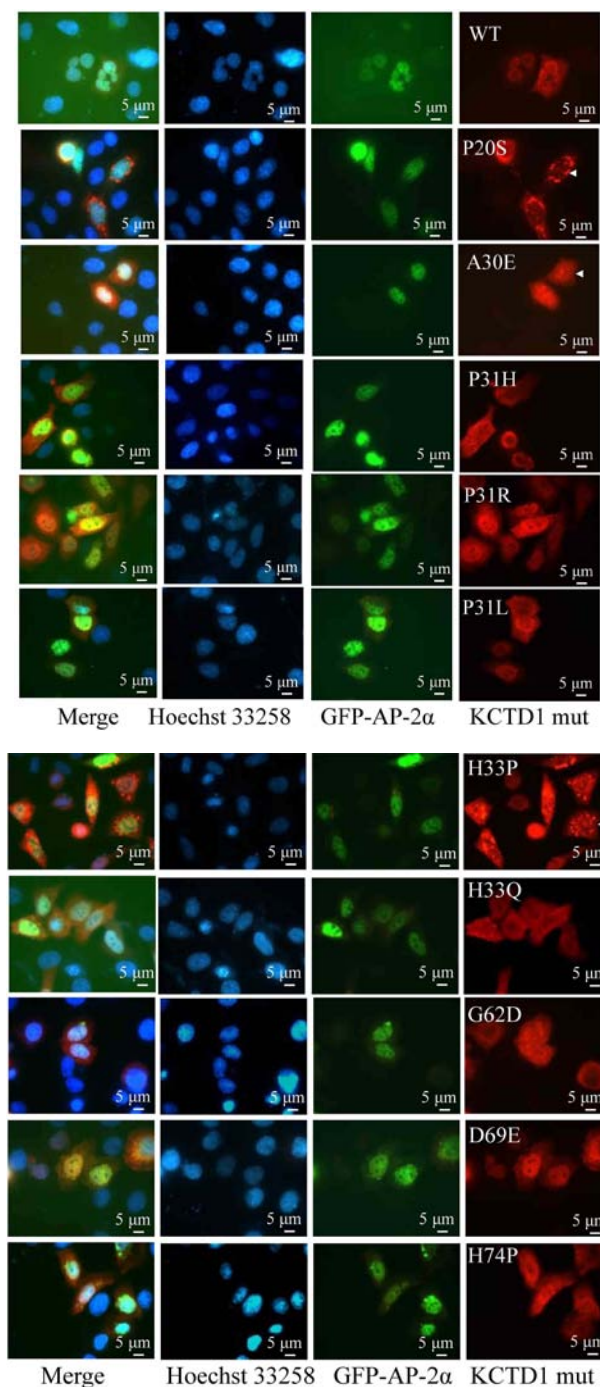


Figure 2. Cellular localization of KCTD1 mutants. HeLa cells were transiently transfected with the expression plasmids pEGFP-C1-AP-2 α and pCMV-Myc-wild-type KCTD1 or pCMV-Myc-KCTD1 mutants. (A) Localization of wild-type AP-2 α and wild-type KCTD1 or KCTD1 mutants including P20S, A30E, P31R, P31L, P31H. (B) Localization of wild-type AP-2 α and KCTD1 mutants including H33P, H33Q, G62D, D69E and H74P. Images were captured at 36 h after transfection. Green, GFP-AP-2 α expression; blue, Hoechst 33258 nuclear stain; red, KCTD1 WT and mutants; yellow indicates overlapping expression. GFP, green fluorescent protein; KCTD1, potassium-channel tetramerization-domain-containing 1; mut, mutant; wt, wild-type.

Altered cellular localization of KCTD1 and AP-2 α mutants, compared with wild-type. Plasmids encoding mutant KCTD1 and AP-2 α proteins were transfected into 293 cells to investigate the localization of both mutant proteins using immunofluorescence (Figs. 2 and 3, respectively). It was

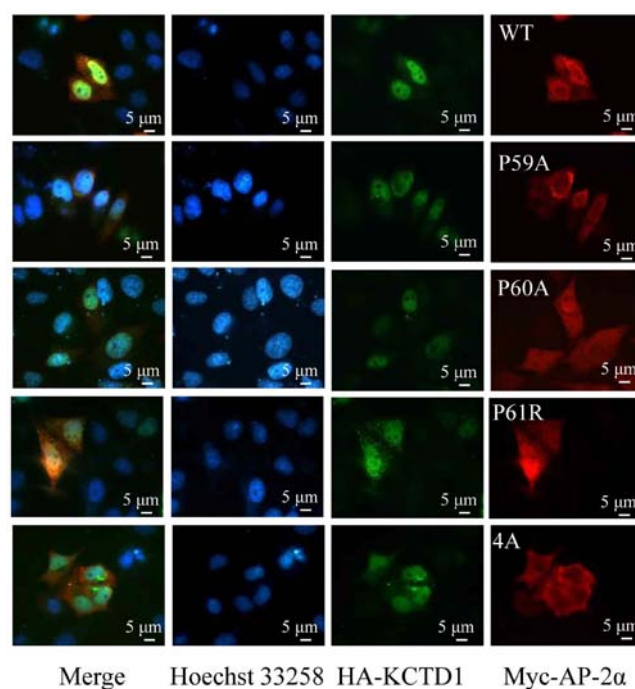


Figure 3. Localization of AP-2 α mutant protein expression. Overexpression of pCMV-HA-KCTD1 and pCMV-Myc-AP-2 α mutants in HeLa cells was assessed by immunofluorescence analysis. Red, AP-2 α ; green, KCTD1; blue, Hoechst 33258 nuclear stain; yellow indicates overlapping expression. KCTD1, potassium-channel tetramerization-domain-containing 1; WT, wild-type.

observed that wild-type KCTD1 localized with wild-type AP-2 α , consistent with previously reported results (13). The KCTD1 mutants (A30E, P31R, P31L, H33Q, G62D, D69E and H74P) were distributed throughout the whole cell, predominantly exhibited strong fluorescence in the nucleus, and co-localized with AP-2 α (Fig. 2). However, localization of KCTD1 P20S was detected in the nuclear membrane. KCTD1 P31H was localized in the nuclear membrane and the cytoplasm (Fig. 2A). KCTD1 H33P clustered in an aggregated pattern in a significant portion of the cells (Fig. 2B). These data suggested that wild-type KCTD1 and its mutant proteins primarily localized in the nucleus, but KCTD1 mutants with mutated amino acids 20 and 31 localized to the nuclear membrane. In addition, wild-type AP-2 α and mutant P60A and P61R protein appeared to demonstrate strong fluorescence in the nucleus and co-localized with KCTD1 protein. However, the AP-2 α P59A and 4A proteins were predominantly detected in the cytoplasm and showed no overlap with KCTD1 protein (Fig. 3). These observations were indicative of altered localization of KCTD1 and AP-2 α .

Protein interactions are altered between KCTD1 mutants/wild-type AP-2 α and wild-type KCTD1/AP-2 α P59A mutant. Coimmunoprecipitation analysis was performed to investigate *in vitro* interactions between AP-2 α and KCTD1 mutants. Anti-KCTD1 antibodies immunoprecipitated the wild-type KCTD1/AP-2 α complex but did not precipitate the KCTD1 mutant/AP-2 α protein complex (Fig. 4A-C). Moreover, consistent with luciferase assay results, KCTD1 formed a complex with AP-2 α P60A and P61R, but not with AP-2 α P59A or 4A (Fig. 4D). These results demonstrated that

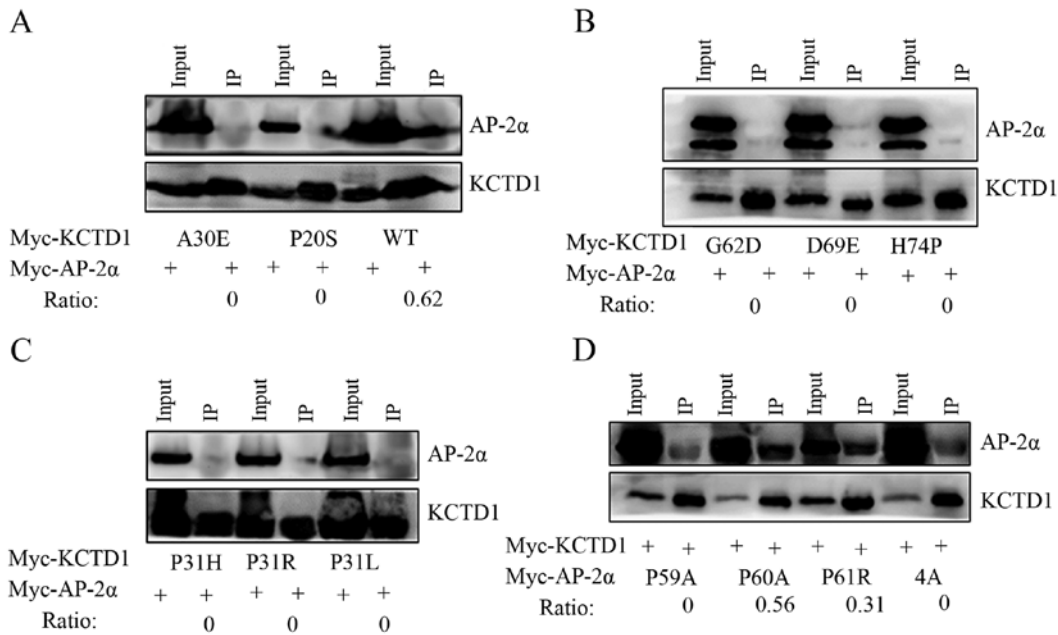


Figure 4. Interaction between KCTD1 and AP-2 α mutants *in vivo*. 293 cells were transiently transfected with expression vectors Myc-AP-2 α and Myc-KCTD1 or their mutants for 30 h. (A) Co-IP of wild-type AP-2 α and wild-type KCTD1 or KCTD1 mutants including A30E and P20S. (B) Co-IP of wild-type AP-2 α and KCTD1 mutants including G62D, D69E and H74P. (C) Co-IP of wild-type AP-2 α and KCTD1 mutants including P31H, P31R and P31L. (D) Co-IP of wild-type KCTD1 and AP-2 α mutants including P59A, P60A, P61R and 4A. Whole-cell extracts were analyzed using mouse monoclonal anti-Myc antibody to confirm protein overexpression and were immunoprecipitated with rabbit polyclonal antibody against KCTD1. Immunoprecipitates were detected by western blotting using mouse monoclonal anti-Myc tag antibody. Pre-immune rabbit IgG served as the negative control. Quantification of bands was analyzed using ImageJ software. Ratio of AP-2 α /KCTD1 indicates the amount of immunoprecipitated AP-2 α proteins relative to the amount of immunoprecipitated KCTD1 proteins. IP, immunoprecipitation; KCTD1, potassium-channel tetramerization-domain-containing 1.

the KCTD1 mutants did not interact with AP-2 α , although some nucleic co-localization was observed for the AP-2 α and KCTD1 mutants, which indicated that KCTD1 mutations in the BTB domain reduce its suppressive effects on AP-2 α . However, KCTD1 continued to inhibit the transcriptional activation of AP-2 α P60A and P61R and formed a complex through protein-protein interaction.

Differential regulation of KCTD1 and AP-2 α mutants on the Wnt/ β -catenin signaling pathway. Wnt/ β -catenin signaling serves a key role in embryonic development and various diseases including bone disease including osteoporosis-pseudoglioma syndrome, cardiometabolic disease and Parkinson's disease (22-25). The present study investigated the effects of KCTD1 mutants on the canonical Wnt/ β -catenin signaling pathway. The TOPFLASH reporter plasmid was transfected into 293 cells in the presence or absence of pCMV-Myc-KCTD1 wild-type or KCTD1 mutants. The results demonstrated that wild-type KCTD1 overexpression markedly suppressed the Wnt pathway-responsive TOPFLASH reporter gene activity (Fig. 5A). In addition, the majority of KCTD1 mutants strongly inhibited the transcriptional activity of the TOPFLASH reporter. KCTD1 A30E or H33Q mutants had no effect on the transcriptional activity of the TOPFLASH reporter, but eight other KCTD1 mutants significantly decreased the transcription activity of the TOPFLASH reporter gene to a similar extent as the wild-type KCTD1. In the H33Q KCTD1 mutant, the change from polar and charged His33 to a polar residue, Gln (Q), did not inhibit TOPFLASH reporter activity. By contrast, the change from His to Pro in the H33P mutant inhibited the TOPFLASH reporter activity. Collectively, these

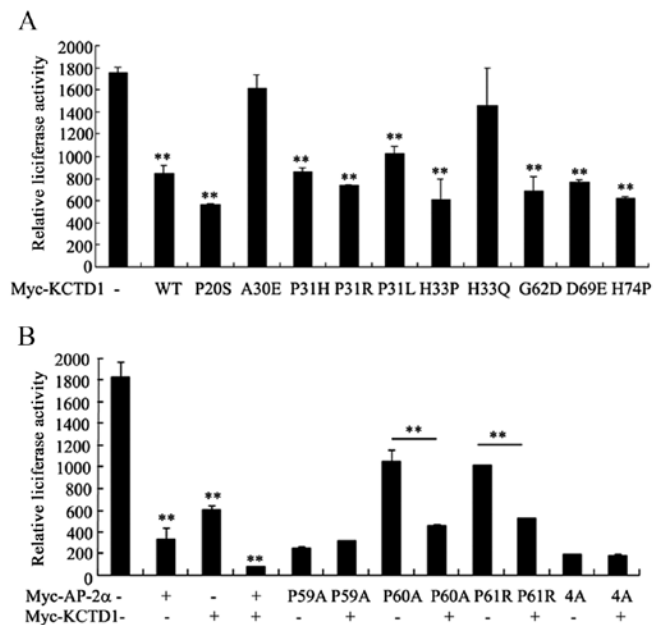


Figure 5. (A and B) Effects of KCTD1 and AP-2 α mutations on TOPFLASH luciferase reporter activity. 293 cells were transiently transfected with the TOPFLASH Wnt luciferase reporter and the indicated expression plasmids. At 24 h after transfection, luciferase and β -galactosidase activity was assayed. Relative luciferase activity is expressed as the mean \pm SD of three independent experiments normalized to β -galactosidase activity. **P<0.01. KCTD1, potassium-channel tetramerization-domain-containing 1; WT, wild-type.

results suggested that Ala 30 and His 33 were important for KCTD1-mediated regulation of Wnt/ β -catenin signaling (Fig. 5A). These data indicate that the pathogenic mechanisms

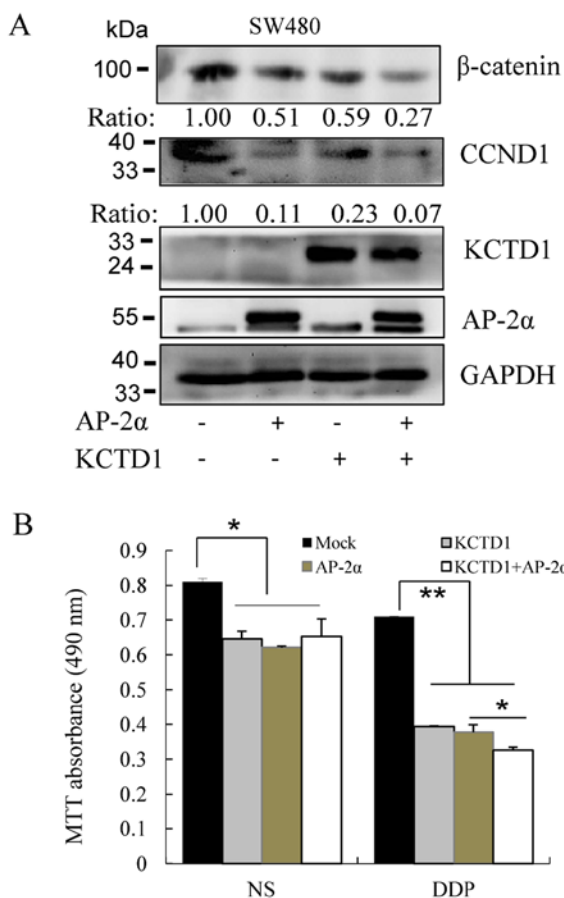


Figure 6. KCTD1 and AP-2 α decrease SW480 cell viability by downregulating β -catenin expression levels. (A) SW480 cells were transiently transfected with pCMV-Myc (Mock), pCMV-Myc-KCTD1 and/or pCMV-Myc-AP-2 α plasmids. At 24 h after transfection, total cell lysates were harvested and detected by western blotting using mouse monoclonal antibodies against β -catenin, Myc-tag, CCND1 and GAPDH. GAPDH served as a loading control for protein normalization. (B) Effects of overexpressed KCTD1, AP-2 α or DDP treatment on SW480 cells. SW480 cells were transiently transfected with pCMV-Myc-KCTD1 and/or pCMV-Myc-AP-2 α plasmids and treated with or without 20 μ M DDP for 24 h. Cell viability was determined by MTT assays and absorbance was measured at 490 nm. * P <0.05, ** P <0.01 compared with controls (the Mock group or the AP-2 α group). KCTD1, potassium-channel tetramerization-domain-containing 1; CCND1, cyclin D1; DDP, cisplatin; NS, normal saline.

underlying certain KCTD1 mutants are primarily due to suppressed Wnt/ β -catenin signaling, resulting in specific abnormal phenotypes in SEN syndrome.

AP-2 α has been reported to inhibit TOPFLASH reporter activity in a manner similar to KCTD1 (17,18). AP-2 α P59A and AP-2 α 4A suppressed TOPFLASH activity to a similar degree as wild-type AP-2 α (Fig. 5B); AP-2 α P60A and P61R also partially inhibited TOPFLASH reporter activity. Notably, inhibition of TOPFLASH reporter activity by AP-2 α P60A and P61R was enhanced in cells co-transfected with wild-type KCTD1, but KCTD1 had no effect on the TOPFLASH reporter activity of AP-2 α P59A or 4A (Fig. 5B). These results supported the hypothesis that the AP-2 α P59A mutant downregulates the Wnt/ β -catenin signaling pathway, which is unaffected by KCTD1.

Finally, western blotting was performed to measure the influence of AP-2 α and KCTD1 proteins on the Wnt/ β -catenin pathway. KCTD1 and AP-2 α overexpression (individually

and in combination) decreased β -catenin expression levels (Fig. 6A); downstream CCND1 expression levels were also downregulated. Moreover, KCTD1 and AP-2 α decreased the survival of the SW480 cells, and 20 μ M chemotherapeutic drug cisplatin (DDP) exhibited a stronger inhibitory effect on the viability of SW480 cells transfected with KCTD1 and/or AP-2 α , compared with the normal saline (NS) group (Fig. 6B). These results demonstrated that KCTD1 and AP-2 α downregulated β -catenin expression levels in the canonical Wnt pathway and inhibited SW480 cell viability, suggesting KCTD1 and AP-2 α might regulate these syndromes through the Wnt/ β -catenin pathway.

Discussion

The BTB domain is crucial for transcriptional regulation; proteins with a BTB domain primarily function as transcriptional repressors (26-28). BTB proteins, such as Bcl-6 and promyelocytic leukemia zinc-finger (PLZF), are involved in a number of developmental processes, such as limb formation, gastrulation, ovary morphogenesis, eye development and hematopoietic stem cell fate determination (29-33). The Bcl6 mutant does not interact with co-repressors through its BTB domain, which results in defective B cell proliferation and survival, disrupted formation of germinal centers and suppressed affinity maturation of immunoglobulin (34). Specifically, residues 33-35 form the floor of the pocket and residues 63, 64 and 66-68 form each wall in the secondary structure of PLZF BTB domain (35). All known KCTD mutants in SEN syndrome are caused by missense mutations, and the BTB pocket is formed by a number of residues (3). KCTD1 mutations associated with SEN syndrome abrogate KCTD1 transcriptional repression activity on transcription factor AP-2 α (13). These missense mutations result in the loss of KCTD1 function in a dominant-negative manner. This is consistent with the present study results, which demonstrated that alterations in the KCTD1 BTB domain had no effect on the transcriptional repression of AP-2 α owing to a lack of interaction, despite a degree of co-localization. Notably, the present study revealed that KCTD1 H33P was localized in a punctate pattern in the cells. These findings were consistent with a previous study in which amyloid precursor protein (APP) exhibited a punctate pattern of immunofluorescence indicative of internalization from the cell surface to an endosomal compartment (36), indicating that KCTD1 H33P may serve important roles in internalization by endocytosis. To investigate the function of KCTD1 mutants in maintaining a normal tissue phenotype, as well as the regulatory association between KCTD1 mutants and Wnt/ β -catenin signaling, normal cell lines, such as 293 cells, were selected as previously described (18). The majority of KCTD1 BTB domain mutants suppressed the Wnt/ β -catenin pathway, indicating that substitutions of amino acids in cases of SEN syndrome do not wholly disrupt transcriptional repression caused by BTB domain mutations in KCTD1, although only KCTD1 A30E and H33Q displayed unchanged TOPFLASH reporter activity. It was hypothesized that KCTD1 mutations that cause SEN syndrome may result in abnormal regulation of AP-2 α and developmental defects.

Char syndrome is characterized by patent ductus arteriosus, facial dysmorphism and incurving fifth fingers (37). The PY motif in AP-2 protein family is associated with Char

syndrome as autosomal dominant diseases (7). The PY motif is conserved in the transcription activation domain of AP-2 proteins and KCTD1 binds to this transactivation domain. KCTD1 inhibited the transcriptional activation of AP-2 α by three-fold, whereas KCTD1 only suppressed the transcriptional activity of AP-2 α P60A and P61R by one-half, and did not decrease the transcriptional activity of AP-2 α P59A (Fig. 1D), indicating that regulatory the AP-2 α mutation could be influenced by differential regulation of KCTD1.

The Wnt/ β -catenin signaling pathway serves a key role in embryonic developmental processes (22,38,39) and carcinogenesis (40-42). Truncations in APC are frequently found in familial adenomatous polyposis, a dominantly inherited disease characterized by polyps in the colon and rectum (43,44). Mutations in β -catenin and APC cause sporadic colon cancer and other types of tumor, such as liver cancer and intraductal papillary neoplasms of the bile duct (45-47). KCTD1 directly binds to β -catenin, enhances its degradation and inhibits the canonical Wnt/ β -catenin signaling pathway (18). In the present study, AP-2 α and KCTD1 downregulated β -catenin expression levels in individual transfection experiments and decreased SW480 cell viability, although both of these proteins exhibited stronger inhibitory effects on β -catenin protein levels and cell viability in co-transfection experiments, potentially due to the negative regulatory association between AP-2 α and KCTD1. The chemotherapy drug cisplatin enhanced the influence of both genes on SW480 cell viability.

In summary, the present data demonstrated that KCTD1 mutants causing SEN syndrome did not bind AP-2 α and exhibited no inhibitory effects on AP-2 α , and that KCTD1 was not associated with AP-2 α P59A-induced Char syndrome. The interactions between KCTD1 mutants/wild-type AP-2 α or wild-type KCTD1/AP-2 α mutants were abrogated as a potential effect of altered localization, including KCTD1 mutants P20S, P31H, H33P and AP-2 α mutants P59A and 4A. However, the majority of KCTD1 and AP-2 α mutants inhibited TOPFLASH reporter activity to different extents, and wild-type KCTD1 and AP-2 α downregulated β -catenin expression levels and decreased SW480 cell viability. Further investigation using an animal model is required to fully elucidate the regulatory mechanisms of these proteins in SEN and Char syndrome.

Acknowledgements

The authors would like to thank Dr Limin Li (Hunan Normal University, Changsha, China) for critical editing of the manuscript.

Funding

The present study was supported by The National Natural Science Foundation of China (grant no. 81872256, 81770389 and 81272190), and The Cooperative Innovation Center of Engineering and New Products for Developmental Biology of Hunan Province (grant no. 20134486).

Availability of data and materials

The datasets used and analyzed during this study are available from the corresponding author on reasonable request.

Authors' contributions

XD designed the present study and wrote the manuscript. LH, LC, WH, ZY, LY, XL, QL and JQ performed the experiments and analyzed the data. All authors read and approved the final version of the manuscript.

Ethics approval and consent to participate

Not applicable.

Patient consent for publication

Not applicable.

Competing interests

The authors declare that they have no competing interests.

References

1. Finlay AY and Marks R: An hereditary syndrome of lumpy scalp, odd ears and rudimentary nipples. *Br J Dermatol* 99: 423-430, 1978.
2. van Steensel MA, Celli J, van Bokhoven JH and Brunner HG: Probing the gene expression database for candidate genes. *Eur J Hum Genet* 7: 910-919, 1999.
3. Marneros AG, Beck AE, Turner EH, McMillin MJ, Edwards MJ, Field M, de Macena Sobreira NL, Perez ABA, Fortes JAR, Lampe AK, *et al*: Mutations in KCTD1 cause scalp-ear-nipple syndrome. *Am J Hum Genet* 92: 621-626, 2013.
4. Zhang J, Hagopian-Donaldson S, Serbedzija G, Elsemore J, Plehn-Dujowich D, McMahon AP, Flavell RA and Williams T: Neural tube, skeletal and body wall defects in mice lacking transcription factor AP-2. *Nature* 381: 238-241, 1996.
5. Ahituv N, Erven A, Fuchs H, Guy K, Ashery-Padan R, Williams T, de Angelis MH, Avraham KB and Steel KP: An ENU-induced mutation in AP-2alpha leads to middle ear and ocular defects in doxrad mice. *Mamm Genome* 15: 424-432, 2004.
6. Sletten LJ and Pierpont ME: Familial occurrence of patent ductus arteriosus. *Am J Med Genet* 57: 27-30, 1995.
7. Zhao F, Weismann CG, Satoda M, Pierpont ME, Sweeney E, Thompson EM and Gelb BD: Novel TFAP2B mutations that cause char syndrome provide a genotype-phenotype correlation. *Am J Hum Genet* 69: 695-703, 2001.
8. Li H, Sheridan R and Williams T: Analysis of TFAP2A mutations in branchio-oculo-facial syndrome indicates functional complexity within the AP-2 α DNA-binding domain. *Hum Mol Genet* 22: 3195-3206, 2013.
9. Milunsky JM, Maher TA, Zhao G, Roberts AE, Stalker HJ, Zori RT, Burch MN, Clemens M, Mulliken JB, Smith R and Lin AE: TFAP2A mutations result in branchio-oculo-facial syndrome. *Am J Hum Genet* 82: 1171-1177, 2008.
10. Milunsky JM, Maher TM, Zhao G, Wang Z, Mulliken JB, Chitayat D, Clemens M, Stalker HJ, Bauer M, Burch M, *et al*: Genotype-phenotype analysis of the branchio-oculo-facial syndrome. *Am J Med Genet A* 155A: 22-32, 2011.
11. Dumitrescu AV, Milunsky JM, Longmuir SQ and Drack AV: A family with branchio-oculo-facial syndrome with primarily ocular involvement associated with mutation of the TFAP2A gene. *Ophthalmic Genet* 33: 100-106, 2012.
12. Thomeer HG, Crins TT, Kamsteeg EJ, Buijsman W, Cruysberg JR, Knoers NV and Cremers CWRJ: Clinical presentation and the presence of hearing impairment in branchio-oculo-facial syndrome: A new mutation in the TFAP2A gene. *Ann Otol Rhinol Laryngol* 119: 806-814, 2010.
13. Ding X, Luo C, Zhou J, Zhong Y, Hu X, Zhou F, Ren K, Gan L, He A, Zhu J, *et al*: The interaction of KCTD1 with transcription factor AP-2alpha inhibits its transactivation. *J Cell Biochem* 106: 285-295, 2009.
14. Zarelli VE and Dawid IB: Inhibition of neural crest formation by Kctd15 involves regulation of transcription factor AP-2. *Proc Natl Acad Sci USA* 110: 2870-2875, 2013.

15. Heffer A, Marquart GD, Aquilina-Beck A, Saleem N, Burgess HA and Dawid IB: Generation and characterization of Kctd15 mutations in zebrafish. *PLoS One* 12: e0189162, 2017.
16. Dutta S and Dawid IB: Kctd15 inhibits neural crest formation by attenuating Wnt/beta-catenin signaling output. *Development* 137: 3013-3018, 2010.
17. Li Q and Dashwood RH: Activator protein 2alpha associates with adenomatous polyposis coli/beta-catenin and inhibits beta-catenin/T-cell factor transcriptional activity in colorectal cancer cells. *J Biol Chem* 279: 45669-45675, 2004.
18. Li X, Chen C, Wang F, Huang W, Liang Z, Xiao Y, Wei K, Wan Z, Hu X, Xiang S, *et al*: KCTD1 suppresses canonical Wnt signaling pathway by enhancing β -catenin degradation. *PLoS One* 9: e94343, 2014.
19. Ding X, Fan C, Zhou J, Zhong Y, Liu R, Ren K, Hu X, Luo C, Xiao S, Wang Y, *et al*: GAS41 interacts with transcription factor AP-2beta and stimulates AP-2beta-mediated transactivation. *Nucleic Acids Res* 34: 2570-2578, 2006.
20. Ding X, Yang Z, Zhou F, Wang F, Li X, Chen C, Li X, Hu X, Xiang S and Zhang J: Transcription factor AP-2 α regulates acute myeloid leukemia cell proliferation by influencing *hoxa* gene expression. *Int J Biochem Cell Biol* 45: 1647-1656, 2013.
21. Ding XF, Luo C, Ren KQ, Zhang J, Zhou JL, Hu X, Liu RS, Wang Y, Gao X and Zhang J: Characterization and expression of a human KCTD1 gene containing the BTB domain, which mediates transcriptional repression and homomeric interactions. *DNA Cell Biol* 27: 257-265, 2008.
22. Clevers H: Wnt/beta-catenin signaling in development and disease. *Cell* 127: 469-480, 2006.
23. Baron R and Kneissel M: WNT signaling in bone homeostasis and disease: From human mutations to treatments. *Nat Med* 19: 179-192, 2013.
24. Gay A and Towler DA: Wnt signaling in cardiovascular disease: Opportunities and challenges. *Curr Opin Lipidol* 28: 387-396, 2017.
25. Ng L, Kaur P, Bunnag N, Suresh J, Sung ICH, Tan QH, Gruber J and Tolwinski NS: WNT signaling in disease. *Cells* 8: 826, 2019.
26. Li X, Peng H, Schultz DC, Lopez-Guisa JM, Rauscher FJ III and Marmorstein R: Structure-function studies of the BTB/POZ transcriptional repression domain from the promyelocytic leukemia zinc finger oncoprotein. *Cancer Res* 59: 5275-5282, 1999.
27. Fedele M, Benvenuto G, Pero R, Majello B, Battista S, Lembo F, Vollono E, Day PM, Santoro M, Lania L, *et al*: A novel member of the BTB/POZ family, PATZ, associates with the RNF4 RING finger protein and acts as a transcriptional repressor. *J Biol Chem* 275: 7894-7901, 2000.
28. Hoatlin ME, Zhi Y, Ball H, Silvey K, Melnick A, Stone S, Arai S, Hawe N, Owen G, Zelent A and Licht JD: A novel BTB/POZ transcriptional repressor protein interacts with the fanconi anemia group C protein and PLZF. *Blood* 94: 3737-3747, 1999.
29. Kelly KF and Daniel JM: POZ for effect--POZ-ZF transcription factors in cancer and development. *Trends Cell Biol* 16: 578-587, 2006.
30. Kojima S, Hatano M, Okada S, Fukuda T, Toyama Y, Yuasa S, Ito H and Tokuhsa T: Testicular germ cell apoptosis in Bcl6-deficient mice. *Development* 128: 57-65, 2001.
31. Shaffer AL, Yu X, He Y, Boldrick J, Chan EP and Staudt LM: BCL-6 represses genes that function in lymphocyte differentiation, inflammation, and cell cycle control. *Immunity* 13: 199-212, 2000.
32. Barna M, Hawe N, Niswander L and Pandolfi PP: Plzf regulates limb and axial skeletal patterning. *Nat Genet* 25: 166-172, 2000.
33. Costoya JA, Hobbs RM, Barna M, Cattoretti G, Manova K, Sukhwani M, Orwig KE, Wolgemuth DJ and Pandolfi PP: Essential role of Plzf in maintenance of spermatogonial stem cells. *Nat Genet* 36: 653-659, 2004.
34. Huang C, Hatzi K and Melnick A: Lineage-specific functions of Bcl-6 in immunity and inflammation are mediated by distinct biochemical mechanisms. *Nat Immunol* 14: 380-388, 2013.
35. Ahmad KF, Engel CK and Prive GG: Crystal structure of the BTB domain from PLZF. *Proc Natl Acad Sci USA* 95: 12123-12128, 1998.
36. Carey RM, Balcz BA, Lopez-Coviella I and Slack BE: Inhibition of dynamin-dependent endocytosis increases shedding of the amyloid precursor protein ectodomain and reduces generation of amyloid beta protein. *BMC Cell Biol* 6: 30, 2005.
37. Char F: Peculiar facies with short philtrum, duck-bill lips, ptosis and low-set ears-a new syndrome? *Birth Defects Orig Artic Ser* 14: 303-305, 1978.
38. Marston DJ, Roh M, Mikels AJ, Nusse R and Goldstein B: Wnt signaling during *Caenorhabditis elegans* embryonic development. *Methods Mol Biol* 469: 103-111, 2008.
39. Munoz-Descalzo S, Hadjantonakis AK and Arias AM: Wnt/ β -catenin signalling and the dynamics of fate decisions in early mouse embryos and embryonic stem (ES) cells. *Semin Cell Dev Biol* 47-48: 101-109, 2015.
40. Wang B, Tian T, Kalland KH, Ke X and Qu Y: Targeting Wnt/ β -catenin signaling for cancer immunotherapy. *Trends Pharmacol Sci* 39: 648-658, 2018.
41. Wang W, Smits R, Hao H and He C: Wnt/ β -catenin signaling in liver cancers. *Cancers (Basel)* 11: 926, 2019.
42. Jung YS and Park JI: Wnt signaling in cancer: Therapeutic targeting of Wnt signaling beyond β -catenin and the destruction complex. *Exp Mol Med* 52: 183-191, 2020.
43. Nishisho I, Nakamura Y, Miyoshi Y, Miki Y, Ando H, Horii A, Koyama K, Utsunomiya J, Baba S and Hedge P: Mutations of chromosome 5q21 genes in FAP and colorectal cancer patients. *Science* 253: 665-669, 1991.
44. Nakamura Y, Nishisho I, Kinzler KW, Vogelstein B, Miyoshi Y, Miki Y, Ando H, Horii A and Nagase H: Mutations of the adenomatous polyposis coli gene in familial polyposis coli patients and sporadic colorectal tumors. *Princess Takamatsu Symp* 22: 285-292, 1991.
45. Suraweera N, Robinson J, Volikos E, Guenther T, Talbot I, Tomlinson I and Silver A: Mutations within Wnt pathway genes in sporadic colorectal cancers and cell lines. *Int J Cancer* 119: 1837-1842, 2006.
46. Colnot S: Focusing on beta-catenin activating mutations to refine liver tumor profiling. *Hepatology* 64: 1850-1852, 2016.
47. Fujikura K, Akita M, Ajiki T, Fukumoto T, Itoh T and Zen Y: Recurrent mutations in APC and CTNNB1 and activated Wnt/ β -catenin signaling in intraductal papillary neoplasms of the bile duct: A whole exome sequencing study. *Am J Surg Pathol* 42: 1674-1685, 2018.



This work is licensed under a Creative Commons Attribution-NonCommercial-NoDerivatives 4.0 International (CC BY-NC-ND 4.0) License.